




Digital Receipt

This receipt acknowledges that Turnitin received your paper. Below you will find the receipt information regarding your submission.

The first page of your submissions is displayed below.

Submission author: Mohamad Jahja, Christoph Bubeck
Assignment title: For writers
Submission title: NONLINEAR OPTICAL WAVEGUID...
File name: 10_Jahja_NLO_Waveguide_Spectro...
File size: 473.89K
Page count: 13
Word count: 4,758
Character count: 22,899
Submission date: 26-Aug-2019 08:12PM (UTC-0700)
Submission ID: 1163860134

Journal of Nonlinear Optical Physics & Materials
Vol. 19, No. 2 (2010) 269–280
© World Scientific Publishing Company
DOI: 10.1142/S0218863510005200

 World Scientific
www.worldscientific.com

NONLINEAR OPTICAL WAVEGUIDE SPECTROSCOPY
OF POLY(3-BUTYLTHIOPHENE)

MOHAMAD JAHJA* and CHRISTOPH BUBECK†
*Maz Planck Institute for Polymer Research, Ackermannweg 10,
D-55128, Mainz, Germany*
**Department of Physics, Gorontalo State University,
Jl. Jend. Sudirman no 9 Gorontalo, Indonesia
†bubeck@mpip-mainz.mpg.de*

Received 19 May 2010

We prepared thin films of the conjugated polymer poly(3-butylthiophene) by spin-coating and performed transmission and reflection spectroscopy to characterize the dispersion of linear refractive index and absorption coefficient at in-plane polarization. Slab waveguides of this regioaradon polythiophene derivative have mode propagation losses smaller than 1 dB/cm at wavelengths larger than 1000 nm. We determined the nonlinear refractive index and two-photon absorption of slab waveguides by means of intensity-dependent prism coupling using picosecond laser pulses in the range 700–1300 nm. These data yield the dispersion of the figures of merit, which appear promising for all-optical waveguide switching at wavelengths larger than 1200 nm.

Keywords: Polythiophene; conjugated polymer; slab waveguide; intensity-dependent prism coupling; nonlinear refractive index; two-photon absorption; figures of merit; all-optical switching.

1. Introduction

Waveguides are basic modules for integrated optics and all-optical switching devices.^{1–5} The switching of light by light is generally based on the non-linearities of the refractive index n or the absorption coefficient α . Their dependencies on light intensity I are commonly expressed by

$$n = n_0 + n_2 I \quad (1)$$

and

$$\alpha = \alpha_0 + \alpha_2 I, \quad (2)$$

where n_0 and α_0 refer to the linear refractive index and absorption coefficient at low intensity, respectively. The nonlinear refractive index n_2 and the nonlinear absorption coefficient α_2 are proportional to the real and imaginary parts of the complex third-order susceptibility $\chi^{(3)}$, respectively.^{6,7} Polymers with a highly

269

NONLINEAR OPTICAL WAVEGUIDE SPECTROSCOPY OF POLY(3- BUTYLTHIOPHENE)

by Mohamad Jahja, Christoph Bubeck

Submission date: 26-Aug-2019 08:12PM (UTC-0700)

Submission ID: 1163860134

File name: 10_Jahja_NLO_Waveguide_Spectroscopy_of_Poly_3_Butylthiophene.pdf (473.89K)

Word count: 4758

Character count: 22899

2
NONLINEAR OPTICAL WAVEGUIDE SPECTROSCOPY
OF POLY(3-BUTYLTHIOPHENE)

1
MOHAMAD JAHJA* and CHRISTOPH BUBECK†

Max Planck Institute for Polymer Research, Ackermannweg 10,
D-55128, Mainz, Germany

*Department of Physics, Gorontalo State University,
Jl. Jend. Sudirman no 6 Gorontalo, Indonesia

†bubeck@mpip-mainz.mpg.de

Received 19 May 2010

4
We prepared thin films of the conjugated polymer poly(3-butylthiophene) by spin-coating and performed transmission and reflection spectroscopy to characterize the dispersion of linear refractive index and absorption coefficient at in-plane polarization. Slab waveguides of this random polythiophene derivative have mode propagation losses smaller than 1 dB/cm at wavelengths larger than 1000 nm. We determined the nonlinear refractive index and two-photon absorption of slab waveguides by means of intensity-dependent prism coupling using picosecond laser pulses in the range 700–1300 nm. These data yield the dispersion of the figures of merit, which appear promising for all-optical waveguide switching at wavelengths larger than 1200 nm.

Keywords: Polythiophene; conjugated polymer; slab waveguide; intensity-dependent prism coupling; nonlinear refractive index; two-photon absorption; figures of merit; all-optical switching.

1. Introduction

Waveguides are basic modules for integrated optics and all-optical switching devices.^{1–5} The switching of light by light is generally based on the non-linearities of the refractive index n or the absorption coefficient α . Their dependencies on light intensity I are commonly expressed by

$$n = n_0 + n_2 I \quad (1)$$

and

$$\alpha = \alpha_0 + \alpha_2 I, \quad (2)$$

2
where n_0 and α_0 refer to the linear refractive index and absorption coefficient at low intensity, respectively. The nonlinear refractive index n_2 and the nonlinear absorption coefficient α_2 are proportional to the real and imaginary parts of the complex third-order susceptibility $\chi^{(3)}$, respectively.^{6,7} Polymers with a highly

delocalized π -electron system along their backbone have gained much interest in recent years, because they exhibit large third-order optical non-linearities.^{8,9} In particular, the nonlinear optical properties of polythiophenes have been investigated with many characterization methods such as third-harmonic generation,^{10–13} degenerate four-wave mixing,^{14–17} Z-scan,^{18–20} two-photon absorption (TPA) induced fluorescence,^{21–24} and model calculations as well.^{25,26} However, the nonlinear optical data of polythiophenes are still not completely known in the near infrared (NIR) to estimate the application criteria for all-optical waveguide switching devices, which are expressed by so-called figures of merit.^{2–5} This would require the determination of all data presented in Eqs. (1) and (2) at particular laser wavelengths λ in the NIR range of 800–1500 nm, respectively.

Intensity-dependent prism coupling turned out as a suitable characterization method of slab waveguides to determine the signs and absolute values of n_0 , n_2 , α_0 , and α_2 , i.e., without the need for reference materials.^{27,28} Recently, the conjugated model polymer MEH-PPV was investigated with intensity-dependent prism coupling and its figures of merit are most promising in the range of 1100–1200 nm at the low-energy tail of its two-photon absorption.^{28–30}

We selected the regiorandom poly(3-butylthiophene), abbreviated P3BT (see Fig. 1(a) for its chemical structure) to perform nonlinear optical waveguide spectroscopy, because P3BT has a sufficiently high glass transition temperature and is suitable for preparing slab waveguides with small mode propagation losses. This paper aims to present our measurements of the linear and nonlinear optical data by means of intensity-dependent prism coupling to evaluate the figures of merit in the NIR range and to clarify their spectral dependence.

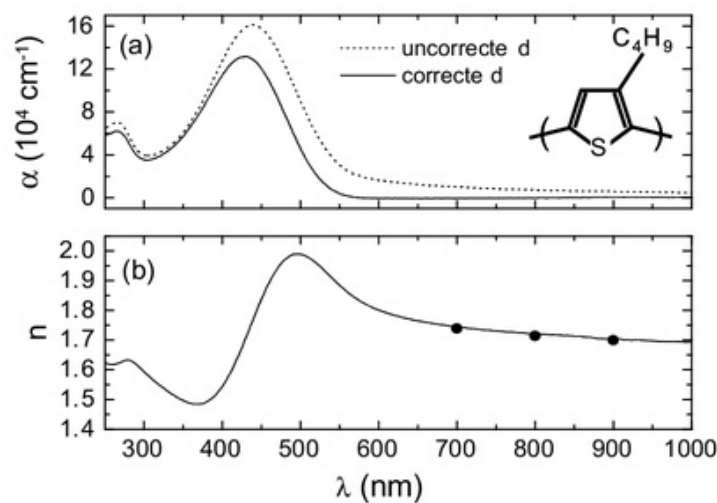


Fig. 1. Chemical structure of P3BT and (a) spectra of absorption coefficient α and (b) refractive index n of $2\text{ }\mu\text{m}$ films measured at TE polarization. The absorption coefficient is displayed as determined relative to fused silica (uncorrected, dashed line) and after correction of reflection losses at interfaces (corrected, full line). Lines are from reflectometry experiments (film thickness $d = 48 \text{ nm}$). Data points are from prism coupling experiments at TE polarization (full circles) using slab waveguides ($d = 535 \text{ nm}$).

2. Experimental Details

2.1. Materials and film preparation

Regiorandom poly(3-butylthiophene), abbreviated P3BT, was purchased from Rieke-Metals and used without further treatment. Figure 1(a) shows its chemical structure. Characterizations of molecular weights and glass transition temperature (T_g) were performed at our institute with Gel Permeation Chromatography (GPC) and Differential Scanning Calorimetry (DSC), respectively. P3BT used in this work has weight average molecular weight $M_w = 3.09 \times 10^4$ g/mol, number average molecular weight $M_n = 1.02 \times 10^4$ mol, and $T_g = 60^\circ\text{C}$, respectively.

P3BT films were spin-cast from their freshly prepared and filtered (0.45 μm syringe filters) toluene solutions onto fused silica substrates, which were cleaned in the following sequence: Washing with liquid soap, then rinsing 10 times with purified water (Milli-Q, Millipore), cleaning in an ultrasonic bath with a solution of 1% detergent (Hellmanex, Hellma) in Milli-Q water for 15 minutes, 10 times rinsing in purified water, cleaning with ethanol, and drying the substrate in a flow of nitrogen.

Typical film thicknesses d in the range of 50–70 nm as needed for optical spectroscopy were obtained by using a solution concentration by weight $c_w = 4\%$ and spinning speed $\omega = 1000$ rpm. Waveguides with typical thickness in the range of 500–600 nm were prepared using $c_w = 8\%$ and $\omega \approx 1000$ rpm. Residual solvents after spin-coating were removed by subsequently annealing the samples to 45°C in a vacuum oven for at least 4 hours at slow changes of temperature to avoid stresses in the films. The film thicknesses were measured with a Tencor model P-10 stylus profilometer.

2.2. Linear optical spectroscopy

Transmission and reflection spectra of thin films ($d \approx 50$ nm) were measured by using a UV-Vis-NIR spectrophotometer (Perkin Elmer Model Lambda 900) at in-plane orientation of the electrical field vector of incident light (TE-polarization). The spectra of the refractive index $n(\lambda)$ of the films were obtained by reflectometry at nearly perpendicular incidence and were evaluated by means of Fresnel's equations as described earlier.^{11,31,32}

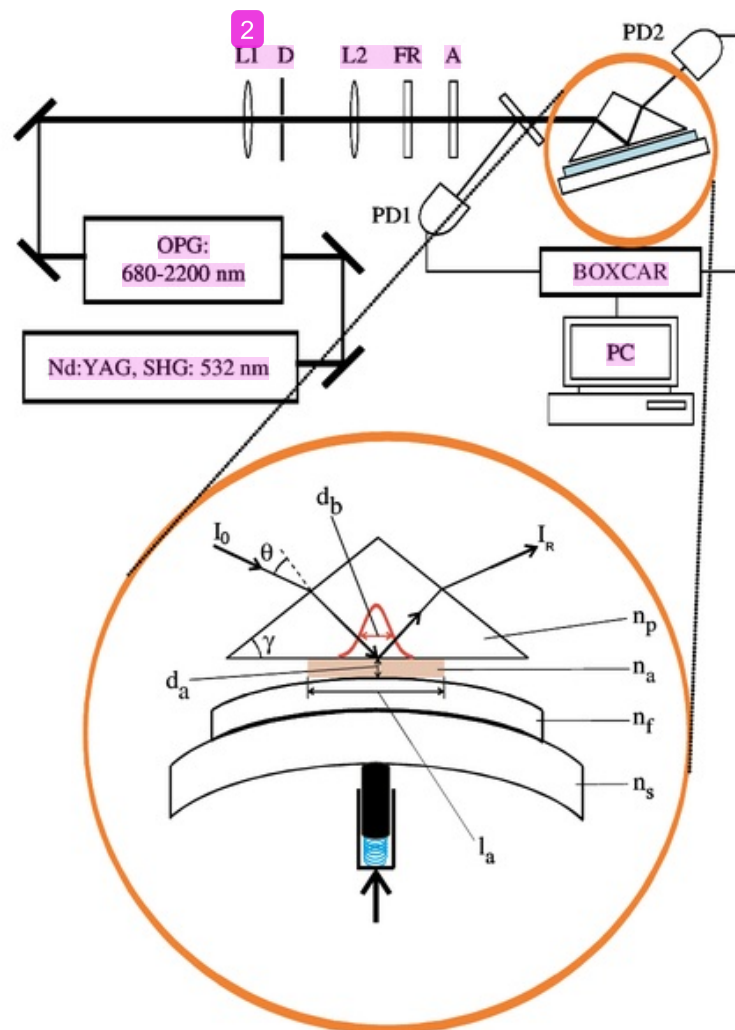
The refractive indices of waveguides at TE-polarization of the electric field vector were determined by prism coupling using the m-line technique^{1,33} and a continuous wave (cw) Nd:YAG laser. The typical thicknesses of waveguides were in the range of 400–800 nm.

Waveguide attenuation loss experiments were performed by use of the cw-Nd:YAG laser at 1064 nm and the set-up described earlier.³⁴ The scattered light from the waveguide mode was imaged by a lens onto a diode array. Attenuation loss coefficients α_{gw} were determined from the scattered light intensity as a function of distance from the coupling prism. The detection limit of this method is in the order of $\alpha_{gw} \approx 0.5$ dB/cm.

2.3. Intensity-dependent prism coupling ⁷

The prism coupler set-up depicted in Fig. 2 was used to measure the nonlinear optical coefficients α_2 and n_2 by intensity-dependent prism coupling as reported recently.^{27,28} Slab waveguides were pressed against the prism base by means of a spring-loaded clamping screw. The prism material was N-LaSF18A Schott glass and the prism angle was $\gamma = 60^\circ$. The prism and photodetector PD2 were mounted on θ and 2θ arms of two-stage goniometers, respectively. Both goniometers are computer controlled and have a precision of 0.01° . Photodetector PD1 was mounted in front of the prism. Both detectors, PD1 and PD2, are InGaAs-type photodiodes.

Second-harmonic output pulses of a Nd:YAG laser (EKSPLA Model PL 2143B) were used to pump an Optical Parametric Generator (OPG, EKSPLA Model



⁶ Fig. 1. Experimental set-up of intensity-dependent prism coupling of slab waveguide ¹ prepared on fused silica substrates, which are pressed against the bottom plane of the prism. A Nd:YAG laser was used, whose second-harmonic ² output (SHG) pumped an optical parametric generator (OPG). Symbol assignments: L1 and L2: lenses; D: spatial filter; FR: Fresnel rhombus; A: polarizer; PD1 and PD2: photodetectors, which are connected to a BOXCAR amplifier; PC: computer. The enlargement shows details of prism coupling and its relevant parameters as explained in the text.

PG501), which has a wavelength tuning range of 680–2000 nm. The typical pulse durations of fundamental laser wavelength 1064 nm and OPG output are 28 ps and 15 ps, respectively, similar to an earlier work.²⁸ Lenses L1 of focal length $f = 8$ cm and L2 ($f = 100$ cm) were used to focus the laser beam onto the prism base involving a spatial filter. The laser beam diameter d_b was measured with a beam profiler (Newport model LBP2-USB2). Typical values are $d_b = 0.4$ – 0.8 mm at the prism base. The intensity of the laser pulses was varied by means of a Fresnel rhombus and a polarizer. Pulse energy was measured with a pyroelectric detector (Laser probe model RjP-735).

Photodiode PD1 was used to measure the relative intensity of incident beam. PD2 detected the reflected signal from the prism base. Signals of both photodetectors were further processed in a BOXCAR amplifier (Stanford Research Systems Model SR250). The problem of laser pulse-to-pulse fluctuations was reduced by selecting and amplifying only such pulses that were located within a narrow energy window at PD1. The normalized reflected intensity I_R was obtained by evaluating the ratio of signals from PD2 and PD1 for each pulse and averaging it over 30–50 pulses.

3. Results

We used transmission and reflection spectroscopy to determine the intrinsic absorption coefficient $\alpha(\lambda)$ and the refractive index n at in-plane (TE) polarization of the electric field vector of incident light. The spectra of $\alpha(\lambda)$ were evaluated from transmission spectra after correction of reflection losses at film/air- and film/substrate-interfaces as described earlier.^{11,31,32} Figure 1(a) shows the spectra $\alpha(\lambda)$ before and after correction of reflection losses. We obtain the intrinsic absorption coefficient $\alpha_{\max} = (1.32 \pm 0.05) \times 10^5 \text{ cm}^{-1}$ and wavelength $\lambda_{\max} = (430 \pm 2) \text{ nm}$ of the maximum of the main absorption band. The experimental error of λ_{\max} is caused by the broad absorption band and the experimental error of α_{\max} is mainly due to the uncertainty of d , respectively. The dispersion of the refractive index n as derived from reflectometry is displayed in Fig. 1(b) together with the results of prism coupling experiments, which are also presented in Table 1. The linear refractive indices from reflectometry and prism coupling show reasonable agreement, i.e., the difference of their refractive indices is smaller than 0.006.

Nonlinear prism coupling occurs when the incident intensity I is so large that the refractive index of the film n_f becomes intensity-dependent. Similarly, the absorption coefficient of the film α_f can also change, e.g. because of increased two-photon absorption. Figure 3 shows an example of intensity-dependent prism coupling. The minimum of the coupling angle θ shifts with increasing energy of the incident laser pulses. This is directly related to a change of n_f . The resonance curve also becomes deeper due to an increase of α_f . The intensity-dependent shifts of the coupling curves were fully reversible, at least using input laser pulse energies up to approximately $1.5 \mu\text{J}$ at $\lambda = 1064 \text{ nm}$. Numerical fits to the measured data were performed

Table 1. Optical constants and figures of merit (W, T) of thin films of P3BT. They were determined with prism coupling at in-plane (TE) polarization using waveguides with a thickness of 535 nm, except for n_0 and α_0 data at $\lambda = 1064$ nm, where the waveguide thickness was 834 nm (see text for symbol definitions). Linear refractive index n_0 and absorption coefficient α_0 at 1064 nm were measured with a low power cw-Nd:YAG laser, the other linear optical data result from extrapolations to zero intensity of the waveguide modes, respectively. The figures of merit W and T are evaluated using an intensity $I = 1 \text{ GW/cm}^2$.

λ [nm]	$n_0 \pm 0.0001$	α_0 [cm^{-1}]	n_2 [cm^2/W]	α_2 [cm/W]	W	T
700	1.7384	3.0 ± 1.0	$(-1.5 \pm 0.2) \times 10^{-13}$	$(3.0 \pm 1.0) \times 10^{-10}$	0.71 ± 0.26	0.28 ± 0.10
800	1.7138	2.0 ± 0.1	$(-3.0 \pm 1.0) \times 10^{-14}$	$(7.0 \pm 1.0) \times 10^{-10}$	0.19 ± 0.06	3.73 ± 1.64
900	1.6996	1.0 ± 0.1	$(4.0 \pm 1.0) \times 10^{-14}$	$(2.0 \pm 0.5) \times 10^{-9}$	0.44 ± 0.12	9.00 ± 3.18
1064	1.68615	0.25 ± 0.1	$(7.0 \pm 1.0) \times 10^{-14}$	$(1.3 \pm 2.0) \times 10^{-9}$	2.19 ± 0.80	3.95 ± 0.83
1100	1.6835	0.2 ± 0.1	$(1.0 \pm 0.1) \times 10^{-13}$	$(1.0 \pm 0.3) \times 10^{-9}$	4.55 ± 2.32	2.20 ± 0.70
1200	1.6827	0.1 ± 0.1	$(2.3 \pm 0.8) \times 10^{-14}$	$(2.0 \pm 1.0) \times 10^{-10}$	1.92 ± 2.09	2.09 ± 1.38
1300	1.6792	0.1 ± 0.1	$(1.5 \pm 1.0) \times 10^{-14}$	$(1.0 \pm 0.5) \times 10^{-10}$	1.15 ± 1.39	1.73 ± 1.44

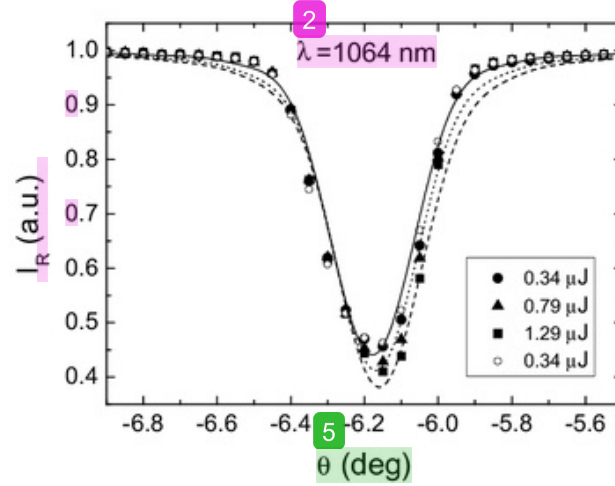


Fig. 3. Coupling curves of TE_0 waveguide modes of a 535 nm thick film of P3BT prepared on a fused silica substrate at the fundamental wavelength of the Nd:YAG laser (1064 nm), that were excited at different pulse energies E measured in front of the prism. The reflected intensity I_R is displayed versus coupling angle θ (compare Fig. 2). The lines are numerical fits to the experimental points using the model reported recently.²⁸ Fit parameters: air gap thickness $d_a = 264$ nm (held constant); refractive index n_f and absorption coefficient α_f of the film were varied to fit the measurements at three energies ($E = 0.34 \mu\text{J}$: $n_f = 1.6862$, $\alpha_f = 1.7 \text{ cm}^{-1}$; $E = 0.79 \mu\text{J}$: $n_f = 1.6863$, $\alpha_f = 3.7 \text{ cm}^{-1}$; $E = 1.29 \mu\text{J}$: $n_f = 1.6864$, $\alpha_f = 5.7 \text{ cm}^{-1}$).

by varying only the two parameters n_f and α_f . The other parameters, such as beam diameter d_b and air-gap thickness d_a were evaluated initially and were held constant in the fitting procedure of the intensity-dependent shifts of the coupling curves as described in detail earlier.²⁸

A crucial step in the evaluation of intensity-dependent prism coupling is the determination of the air-gap thickness d_a between the prism base and film surface, which is accomplished by simulation of the angular-dependence of the reflected intensity I_R at low input energy as described in detail elsewhere.^{27,28} The knowledge of d_a enables the evaluation of the average intensity $\langle I_{gw} \rangle$ in the waveguide.^{27,28} Figure 4 shows examples of the changes of n_f and α_f at 1064 nm as a function of $\langle I_{gw} \rangle$. For comparison with the data of intensity-dependent prism coupling, the results of prism coupling using low power cw-Nd:YAG laser are also shown in Fig. 4. The data of n_f and α_f increase linearly with $\langle I_{gw} \rangle$, which is typical for a third-order nonlinear optical process and allow the evaluation of n_2 and α_2 of the waveguide according to

$$\Delta n_f = n_2 \langle I_{gw} \rangle, \quad (3)$$

$$\Delta \alpha_f = \alpha_2 \langle I_{gw} \rangle. \quad (4)$$

The intensity-dependent prism coupling experiments were performed in the range 700–1300 nm. The results of the linear refractive index n_0 and the linear absorption coefficient α_0 refer to extrapolations of n_f and α_f to the corresponding data at $\langle I_{gw} \rangle = 0$. They are shown in Table 1, together with the evaluated nonlinear optical coefficients n_2 and α_2 , respectively.

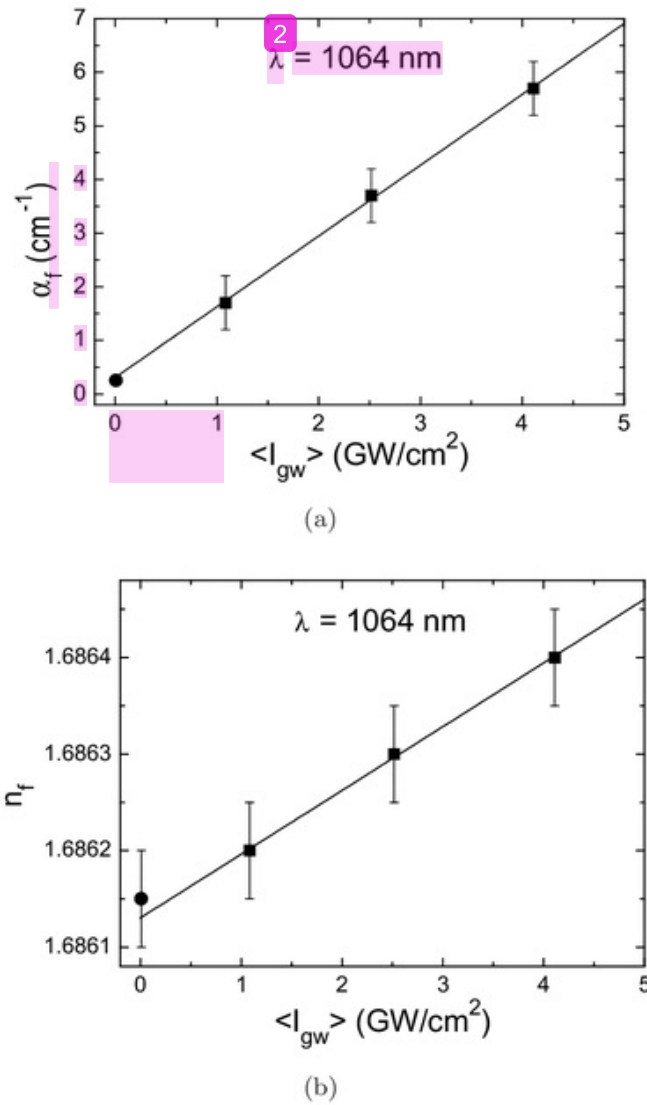


Fig. 4. Intensity dependencies of (a) absorption coefficient α_f and (b) refractive index n_f of a P3BT slab waveguide ($d = 535$ nm) at TE polarization. The average guided wave intensity $\langle I_{gw} \rangle$ is calculated as described previously. The data were measured with intensity-dependent prism coupling squares) and also using a low power cw-Nd:YAG laser (circles, waveguide thickness $d = 834$ nm) as described in the text. The experimental error of α_f at low intensity (full circle) is less than symbol size.

4. Discussion

4.1. Linear optical properties

Inspection of Table 1 reveals that the waveguide losses at TE polarization decrease monotonically from $\alpha_0 = 3$ cm⁻¹ at 700 nm to approximately 0.2 cm⁻¹ and less at $\lambda > 1000$ nm. As the electronic and vibrational absorptions of P3BT are negligible at 600 nm $< \lambda < 1600$ nm, we interpret this decay with Rayleigh and Mie type light scattering and their typical wavelength dependence.³⁵ This shows that region-random P3BT is suitable to prepare slab waveguides with sufficiently low waveguide propagation losses < 1 dB/cm at $\lambda > 1000$ nm.

The refractive index shows normal dispersion at $\lambda > 550$ nm. The results from thin films, determined with reflectometry ($d \approx 50$ nm), and films with $d > 500$ nm investigated with prism coupling yield nearly the same refractive index, i.e., the data of n do not differ more than $\Delta n = 0.006$, which is close to the experimental uncertainty.

4.2. Nonlinear optical properties

We like to point out first that the intensity-dependent changes of n and α observed here have a pure electronic origin, i.e., they are not thermally induced because of the short pulse duration (typically 20 ps) and low repetition rate (10 Hz) of our laser system. Furthermore, these “nonlinearities” would normally show $n_2 < 0$ only.

Inspection of Table 1 shows large two-photon absorption (TPA) of P3BT excited at laser wavelengths of 900–1100 nm, which refers to a TPA energy level at 2.26–2.76 eV. This is in good agreement with earlier reports of TPA in polythiophenes. Using the oligomer α -sexithienyl, Periasamy *et al.* observed several distinct TPA energy levels at 2.25–2.48 eV,²¹ which are close to the TPA level of poly(3-octylthiophene) thin films located at 2.5 eV as reported by Sakurai *et al.*²² Polythiophenes can show a second, higher-energy TPA maximum at approximately 3.5 eV.^{23,24} However, we do not observe this TPA level at 3.5 eV for experimental reasons.

The nonlinear refractive index of P3BT has a maximum $n_2 = 1 \times 10^{-13}$ cm²/W at approximately 1100 nm and decreases monotonically at larger λ . At shorter wavelengths, n_2 becomes zero at approximately $\lambda = 850$ nm and gets a negative sign at $\lambda < 850$ nm. We interpret this dispersion of n_2 by considering the joint occurrence of two electronic processes: TPA as described above, and saturable absorption, which happens if the laser wavelength approaches the tail of the electronic absorption band. Saturation of the exciton absorption in polythiophenes at high laser pulse intensities was already observed earlier.^{14,15,19,20} Kramers–Kronig relations³⁶ and model calculations²⁷ reveal that the dispersions of absorption coefficient and refractive index are strongly correlated to each other. This way, we see a qualitative agreement of the dispersion of n_2 of P3BT with both, the model of Stegeman for a three-level system³⁷ and the dispersion of n_2 of the conjugated polymer MEH-PPV.^{28,30}

4.3. Figures of merit

The materials requirements for all-optical waveguide switching devices can be formulated as so-called figures of merit^{2–5}

$$W = \frac{n_2 I}{\alpha_0 \lambda}, \quad (5)$$

$$T = \frac{2\alpha_2 \lambda}{n_2}. \quad (6)$$

Figures of merit of different materials are usually compared by using a typical intensity $I = 1 \text{ GW/cm}^2$. The application criteria of waveguides for all-optical switching are satisfied if $W > 1$ and $T < 1$.^{2–5} We use the measured values of α_0 , α_2 and n_2 to calculate W and T by means of Eqs. (5) and (6), respectively. The coefficient α_0 also includes the waveguide propagation losses induced by light scattering. Table 1 shows that W reaches a maximum value of $W = 4.5$ at 1100 nm according to the maximum of n_2 and decreases at longer wavelengths. Although our data of T suffer from large experimental errors caused mainly by significant difficulties to determine α_2 with intensity-dependent prism coupling, we observe that T is dominated by the dispersion of TPA. Consequently, we expect that T decreases for $\lambda > 1200 \text{ nm}$ and should not be a limiting factor at longer wavelengths. At $\lambda < 1000 \text{ nm}$, the requirements for the figures of merit cannot be satisfied because of small n_2 values, strongly increasing linear waveguide attenuation losses α_0 , and the possible second TPA maximum at 3.5 eV.^{23,24} We conclude that P3BT is a promising materials candidate for all-optical waveguide-switching applications at $\lambda > 1200 \text{ nm}$.

5. Summary and Conclusion

We prepared thin films of regiorandom poly(3-butylthiophene) (P3BT) and characterized their linear and nonlinear optical properties with reflectometry and intensity-dependent prism coupling using picosecond laser pulses, which were tuned in the wavelength range 700–1300 nm. Our experiments provide the linear and nonlinear optical data α_0 , n_0 , α_2 and n_2 , which are obtained from absolute measurements, as no reference materials are needed.

The linear waveguide attenuation losses α_0 are mainly caused by light scattering, which decrease towards the near-infrared. At $\lambda > 1000 \text{ nm}$, the waveguides have sufficiently low losses $< 1 \text{ dB/cm}$ as needed for waveguide applications in integrated optics.

We observe significant two-photon absorption (TPA) in the order of $\alpha_2 = 1 \text{ cm/GW}$ at laser wavelengths $\lambda = 1100\text{--}1200 \text{ nm}$. This agrees well with earlier reports of TPA in polythiophenes, which locate a TPA energy level at 2.5 eV.^{21,22}

The dispersion of n_2 is dominated by TPA and saturable absorption. The latter process causes a negative sign of n_2 at $\lambda < 800 \text{ nm}$. The dispersion of n_2 is in qualitative agreement with a model calculation of Stegeman involving a three-level system.³⁷ The absolute value of n_2 (1100 nm) = $1 \times 10^{-13} \text{ cm}^2/\text{W}$ is about half of the value reported for the conjugated model polymer MEH-PPV^{28–30} and competes well with silicon, which has n_2 (1270 nm) = $2.6 \times 10^{-14} \text{ cm}^2/\text{W}$.³⁸

We determined the dispersion of the figures of merit, which are the relevant application criteria for all-optical waveguide switching devices. Our results of P3BT thin films are in line with the behavior of the conjugated polymer MEH-PPV, which also shows most promising figures of merit at the low-energy tail of the two-photon absorption. In the spectral region at $\lambda > 1200 \text{ nm}$, the data of n_2 of P3BT are still

resonantly enhanced by TPA, but the waveguide attenuation losses can already be small enough to enable all-optical waveguide switching applications.

1

Acknowledgments

We thank G. Herrmann, W. Scholdei and H. Menges for technical support and the German Academic Exchange Services (DAAD) for the PhD-stipend to M. Jahja, respectively.

1

References

1. P. K. Tien, *Rev. Mod. Phys.* **49** (1977) 361–420.
2. G. I. Stegeman and R. H. Stolen, *J. Opt. Soc. Am. B* **6** (1989) 652–662.
3. G. I. Stegeman, *Proc. SPIE* **1852** (1993) 75–89.
4. A. G. Astill, *Thin Solid Films* **204** (1991) 1–17.
5. J. L. Brédas, C. Adant, P. Tackx and A. Persoons, *Chem. Rev.* **94** (1994) 243–278.
6. P. N. Butcher and D. Cotter, *The Elements of Nonlinear Optics* (Cambridge University Press, Cambridge, 1990).
7. R. W. Boyd, *Nonlinear Optics* (Academic Press, Orlando, 1992).
8. J. Messier, F. Kajzar, P. N. Prasad and D. Ulrich (eds.), *Nonlinear Optical Effects in Organic Polymers* (Kluwer, Dordrecht, 1989).
9. F. Kajzar and J. D. Swalen (eds.), *Organic Thin Films for Waveguiding Nonlinear Optics* (Gordon and Breach Publ., Amsterdam, 1996).
10. D. Neher, A. Wolf, M. LeClerc, A. Kaltbeitzel, C. Bubeck and G. Wegner, *Synth. Met.* **37** (1990) 249–253.
11. A. Mathy, K. Ueberhofen, R. Schenk, H. Gregorius, R. Garay, K. Müllen and C. Bubeck, *Phys. Rev. B* **53** (1996) 4367–4376.
12. H. Kishida, K. Hirota, T. Wakabayashi, H. Okamoto, H. Kokuboc and T. Yamamoto, *Appl. Phys. Lett.* **87** (2005) 121902_1–3.
13. I. Rau, P. Armatys, P.-A. Chollet, F. Kajzar and R. Zamboni, *Mol. Cryst. Liq. Cryst.* **446** (2006) 23–45.
14. R. Dorsinville, L. Yang, R. R. Alfano, R. Zamboni, R. Danieli, G. Ruani and C. Taliani, *Opt. Lett.* **14** (1989) 1321–1323.
15. C. Bubeck, A. Kaltbeitzel, A. Grund and M. LeClerc, *Chem. Phys.* **154** (1991) 343–348.
16. L. Yang, R. Dorsinville, R. R. Alfano, C. Taliani, G. Ruani, R. Zamboni and R. Tubino, *Synth. Met.* **43** (1991) 3197–3200.
17. O. Haba, T. Hayakawa, M. Ueda, H. Kawaguchi and T. Kawazoe, *React. Funct. Polym.* **37** (1998) 163–168.
18. E. Van Keuren, H. Möhwald, S. Rozouvan, W. Schrof, V. Belov, H. Matsuda and S. Yamada, *J. Chem. Phys.* **110** (1999) 3584–3590.
19. E. Van Keuren, T. Wakebe, R. Andraus, H. Möhwald, W. Schrof, V. Belov, H. Matsuda and Raul Rangel-Rojo, *Appl. Phys. Lett.* **75** (1999) 3312–3314.
20. L. Yang, R. Dorsinville, Q. Z. Wang, P. X. Ye, R. R. Alfano, R. Zamboni and C. Taliani, *Opt. Lett.* **17** (1992) 323–325.
21. N. Periasamy, R. Danieli, G. Ruani, R. Zamboni and C. Taliani, *Phys. Rev. Lett.* **68** (1992) 919–922.
22. K. Sakurai, H. Tachibana, N. Shiga, C. Terakura, M. Matsumoto and Y. Tokura, *Phys. Rev. B* **56** (1997) 9552–9556.

23. N. Pfeffer, P. Raimond, F. Charra and J.-M. Nunzi, *Chem. Phys. Lett.* **201** (1993) 357–363.
24. R. K. Meyer, R. E. Benner, Z. V. Vardeny, M. Liess, M. Ozaki, K. Yoshino, Y. Ding and T. Barton, *Synth. Met.* **84** (1997) 549–550.
25. Z. G. Soos and D. S. Galvão, *J. Phys. Chem.* **98** (1994) 1029–1033.
26. M. Das and S. Ramasesha, *J. Chem. Sci.* **118** (2006) 67–78.
27. K. Ueberhofen, A. Deutesfeld, K. Koynov and C. Bubeck, *J. Opt. Soc. Am. B* **16** (1999) 1921–1935.
28. K. Koynov, N. Goutev, F. Fitrilawati, A. Bahtiar, A. Best and C. Bubeck, *J. Opt. Soc. Am. B* **19** (2002) 895–901.
29. M. A. Bader, G. Marowsky, A. Bahtiar, K. Koynov, C. Bubeck, H. Tillmann, H.-H. Hörhold and S. Pereira, *J. Opt. Soc. Am. B* **19** (2002) 2250–2262.
30. A. Bahtiar, K. Koynov, A. Kibrom, T. Ahn and C. Bubeck, *Proc. SPIE* **6330** (2006) 63300C-1–14.
31. R. Schwarz, W. A. Goedel, N. Somanathan, C. Bubeck, U. Scheunemann, W. Hickel and G. Wegner, *Springer Ser. Solid State Sci.* **107** (1992) 337–340.
32. F. Fitrilawati, M.O. Tjia, S. Pfeiffer, H.-H. Hörhold, A. Deutesfeld, H. Eichner and C. Bubeck, *Opt. Mater.* **21** (2002) 511–519.
33. R. Ulrich and R. Torge, *Appl. Opt.* **12** (1973) 2901–2908.
34. A. Mathy, H. U. Simmrock and C. Bubeck, *J. Phys. D: Appl. Phys.* **24** (1991) 1003–1008.
35. H. Ma, A. K.-Y. Jen and L. R. Dalton, *Adv. Mater.* **14** (2002) 1339–1365.
36. D. C. Hutchings, M. Sheik-Bahae, D. J. Hagan and E. W. Van Stryland, *Opt. Quant. Electron.* **24** (1992) 1–30.
37. G. I. Stegeman, *Nonlinear Optics of Organic Molecules and Polymers*, eds. H. S. Nalwa and S. Miyata (CRC Press Inc., Boca Raton, 1997), pp. 799–812.
38. M. Dinu, F. Quochi and H. Garcia, *Appl. Phys. Lett.* **82** (2003) 2954–2956.

Copyright of Journal of Nonlinear Optical Physics & Materials is the property of World Scientific Publishing Company and its content may not be copied or emailed to multiple sites or posted to a listserv without the copyright holder's express written permission. However, users may print, download, or email articles for individual use.

NONLINEAR OPTICAL WAVEGUIDE SPECTROSCOPY OF POLY(3-BUTYLTHIOPHENE)

ORIGINALITY REPORT

33%

SIMILARITY INDEX

25%

INTERNET SOURCES

34%

PUBLICATIONS

1%

STUDENT PAPERS

PRIMARY SOURCES

- 1** phys.unpad.ac.id 10%
Internet Source
- 2** ubm.opus.hbz-nrw.de 9%
Internet Source
- 3** Ayi Bahtiar, Kaloian Koynov, Yati Mardiyati, Hans-Heinrich Hörhold, Christoph Bubeck. "Slab waveguides of poly(p-phenylenevinylene)s for all-optical switching: impact of side-chain substitution", Journal of Materials Chemistry, 2009
Publication 6%
- 4** Yan Jiang, Zulin Da, Fengxian Qiu, Yijun Guan, Guorong Cao. "Fabrication of chromophore molecule-linked azo polymer as waveguide material of polymeric thermo-optic digital optical switch", Journal of Nonlinear Optical Physics & Materials, 2017
Publication 3%
- 5** Jahja, Mohamad. "Thin films of polythiophene: Linear and nonlinear optical characterization", 08: Physik, Mathematik und Informatik. 08: Physik, Mathematik und Informatik, 2011.
Publication 2%
- 6** Bahtiar, Ayi, Kaloian Koynov, Asmorom Kibrom, Taek Ahn, Christoph Bubeck, Kevin D. Belfield, and Francois Kajzar. "", Nonlinear Optical Transmission and Multiphoton Processes in 2%

Organics IV, 2006.

Publication

7

Kaloian Koynov. "Nonlinear prism coupling of waveguides of the conjugated polymer MEH-PPV and their figures of merit for all-optical switching", Journal of the Optical Society of America B, 04/01/2002

1%

Publication

Exclude quotes On

Exclude matches < 1%

Exclude bibliography On